Thermoelectric CMOS Anemometers

F. Mayer, M. Hintermann, H. Jacobs, O. Paul, and H. Baltes

ETH Zürich, Physical Electronics Laboratory, HPT H6, CH-8093 ZURICH, Switzerland

ABSTRACT

We report the fabrication, packaging, and characterization of thermoelectric CMOS anemometers. The sensors are fabricated using the commercial 2 µm CMOS process of EM Microelectronic-Marin SA, Switzerland, followed by bulk silicon micromachining. They consist of a membrane of the CMOS dielectrics heated by integrated polysilicon resistors. Integrated p-polysilicon/n-polysilicon thermopiles detect wind-induced temperature differences on the membrane. Two devices are reported. The first, on a 1 mm by 1.3 mm die, measures one component of the wind velocity. The second structure, on a 2 mm by 2 mm die, measures the modulus and the direction of the air flow. We demonstrate packaging solutions for both sensors. They are mounted on a standard TO substrate, embedded in epoxy, and mechanically protected by a wire-mesh. The performance of the two-dimensional device is enhanced by a flow concentrator. The sensor responses were characterized in a wind-tunnel as a function of sensor orientation, air velocity, and mesh parameters. The output signals grow monotonically with the air velocity up to 40 mV at 38 ms^{-1} (12 Beaufort) at a heating power of 3 mW. Angle detection is demonstrated with standard deviation smaller than 13°. Cost-effective batch production and low power consumption make these thermal devices an interesting alternative to conventional, mechanical, anemometers.

Keywords: anemometer, wind, flow, thermal, thermoelectric, micromachining, CMOS, microsensor

2. INTRODUCTION

There is a growing market for small, accurate instruments allowing to measure the wind force. A variety of such devices are commercialized at prices between 100 and 2000 $. Mainly two operating principles are used. The first is based on the translation of the air momentum into propeller rotation, which is detected optically or inductively [1]. The second method, hot wire anemometry, exploits the cooling of a heated wire by the gas flow. A drawback of the first principle is the robustness required of the mechanical parts, which sets a lower limit to their miniaturization.

Miniaturized thermal gas flow sensors on the other hand have been reported previously [2-9]. Flow sensors can be cost-effectively fabricated by industrial CMOS processes followed by dedicated post-processing micromachining [3,10]. Advantages of analog CMOS technology for the fabrication of such devices include (i) the small attainable size of the structures, (ii) the excellent thermal isolation provided by micromachined dielectric support structures, (iii) a power consumption of only 10^{-3} W, (iv) the straightforward integration of thermopiles, and (v) the possible cointegration of dedicated circuitry.

The response of CMOS gas flow sensors in narrow channels was studied and reported previously [11,12]. The use of such devices for anemometric measurements introduces several new issues. The first concerns the signal level, expected to be significantly lower than that of sensors mounted in narrow flow channels. The second relates to packaging. After mounting on an appropriate substrate, the sensor has to be protected by a robust mechanical barrier which simultaneously has to be partially transparent to air flow. The device response, i.e., its sensitivity and angle dependence, have to be optimized within these packaging constraints.

We report the successful fabrication, packaging, and characterization of anemometers based on CMOS gas flow sensors. As shown schematically in Fig. 1, the sensors are based on a membrane made of the CMOS dielectric layers. An integrated polysilicon resistor plays the role of the hot wire. At two locations on the membrane, A and B, symmetrical with respect to the heater, the membrane temperature is measured. The device exploits the flow velocity dependent heat transfer by the

moving gas. At a flow velocity v, a temperature difference $\Delta T(v)$ builds up between A and B, from which v is determined. By the simultaneous measurement of two temperature asymmetries ΔT_x and ΔT_y on the same chip in perpendicular directions, both components v_x and v_y of the two-dimensional flow vector $v = (v_x, v_y) = (v \cos\Phi, v \sin\Phi)$ are determined. From these, the modulus v and direction Φ of the flow are obtained using $v = (v_x^2 + v_y^2)^{1/2}$ and $\Phi = \arctan(v_y/v_x)$, respectively.

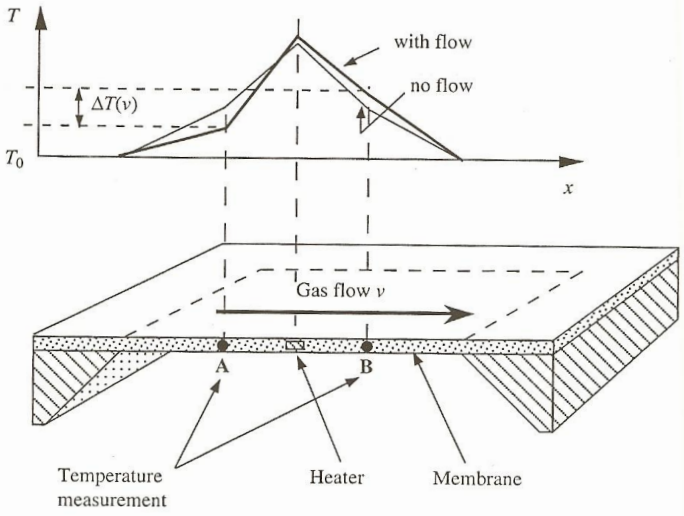

Fig. 1: Operating principle of the thermal CMOS air flow sensors. A heater establishes a temperature profile on the micromachined membrane supported by a frame of silicon. Without flow, the temperature profile is symmetric. Identical temperatures are measured at A and B. With gas flow of velocity v, the temperature difference ΔT(v) is measured.

3. DESIGN AND FABRICATION

We fabricated two different sensors intended, respectively, for one- and two-dimensional operation. Both are based on a membrane made of the entire sandwich of CMOS dielectrics. The sensors were fabricated using the commercial 2 µm CMOS process of EM Microelectronic-Marin SA, Switzerland. After completion of the standard CMOS process, the devices were produced using a one-mask post-processing procedure. First, the front of the devices was protected with 1 µm of tensile PECVD silicon nitride to prevent the membranes from buckling and thereby being damaged. Second, a 0.6 µm thick layer of PECVD silicon nitride was deposited on the back of the substrate and patterned to define the membrane. Finally, the wafers were anisotropically etched from the rear using diluted KOH of density 1.28 g/cm^3 at 95°C. After four hours, the anisotropic etchant reached the etch stop provided by field oxide on the front. During the etch process the front of the devices was mechanically protected. Such processing has already been used to fabricate thermal converters [13,14] and infrared detectors [15-17]. The post-processing produces dielectric membranes supported by rectangular frames of the silicon substrate, as shown schematically in the lower half of Fig. 1.

The one-dimensional sensor is schematically shown in Fig. 2. Its membrane measures 200 µm by 330 µm. The size of the supporting die is 1.0 mm by 1.3 mm. Along its vertical symmetry line, the membrane contains an integrated 4.5 µm wide gate polysilicon line with a resistance of 1.6 kΩ , used as a heater. The heater contacts are placed on the silicon substrate, 30 µm away from the membrane to minimize the influence of the Peltier effect at the heater/metal interface on the sensor response. Temperature increases $(T_A - T_0)$ and $(T_B - T_0)$ of the membrane above the die temperature T_0 are measured at two

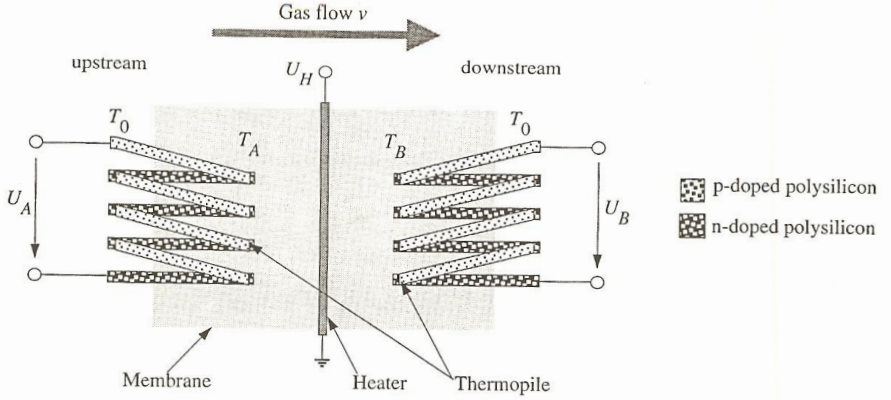

Fig. 2: Schematic top view of CMOS air flow sensor for one-dimensional flow measurements. Heat is generated by a polysilicon line. Temperature differences between T_0 on the die and T_A and T_B on the membrane are measured with integrated bidoped polysilicon thermopiles providing the output signals U_A and U_B.

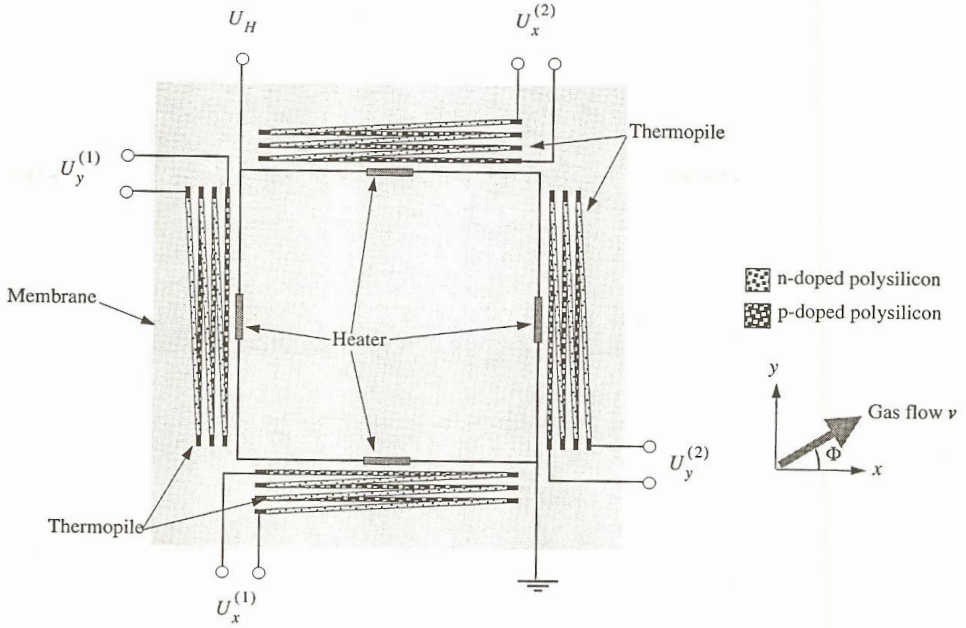

Fig. 3: Schematic top view of CMOS flow sensor for two-dimensional flow measurement. Heat is generated by four polysilicon resistors. Flow-induced temperature differences are measured with four integrated bidoped polysilicon thermopiles. Each pair of parallel thermopiles probes one component of the flow velocity.

symmetrical locations A and B, respectively. These measurements are performed with integrated thermopiles each consisting of 13 bidoped gate-polysilicon/capacitor-polysilicon thermocouples. The hot contacts of the thermopiles are located at a distance of 100 µm from the membrane edge, whereas the cold contacts are placed on the silicon substrate. Respective thermopile output voltages $U_A = 13\alpha(T_A - T_0)$ and $U_B = 13\alpha(T_B - T_0)$ are obtained, where $\alpha = 0.415$ mV/K denotes the Seebeck coefficient of the n-doped gate polysilicon against the p-doped capacitor polysilicon. The voltage difference $U = U_B - U_A$ is a flow-dependent signal with, ideally, zero offset. The internal resistance of the thermopiles is 650 kΩ.

The second sensor is intended for two-dimensional wind velocity measurements. Its membrane measures 600 µm on each side and is supported by a 2 mm by 2 mm large die. The sensor is schematically shown in Fig. 3. Fabrication and characterization of a similar design have been reported previously [9]. Two pairs of integrated thermopiles allow two orthogonal components of the flow velocity to be probed. Each thermopile is composed of six gate-polysilicon/capacitor-polysilicon thermocouples and has a resistance of 450 kΩ . The thermopiles have a length of 300 µm and lie entirely on the membrane. Temperature differences $\Delta T_x^{(1)}$, $\Delta T_x^{(2)}$, $\Delta T_y^{(1)}$, and $\Delta T_y^{(2)}$ on the membrane are measured between the respective thermopile ends. The four output signals $U_x^{(1)} = 6\alpha\Delta T_x^{(1)}$, $U_x^{(2)} = 6\alpha\Delta T_x^{(2)}$, $U_y^{(1)} = 6\alpha\Delta T_y^{(1)}$, and $U_y^{(2)} = 6\alpha\Delta T_y^{(2)}$ are thus obtained. For the characterization, parallel thermopiles are connected in series and the overall thermoelectric signals $U_x = U_x^{(1)} + U_x^{(2)}$ and $U_y = U_y^{(1)} + U_y^{(2)}$ are measured, respectively, for the x and y directions. Heat is generated in four polysilicon resistors of 2.0 kΩ each, located beside the thermopiles.

Photomicrographs of the two sensors are shown in Fig. 4. On both devices, the membrane, thermopiles, heaters, and contact pads can clearly be identified.

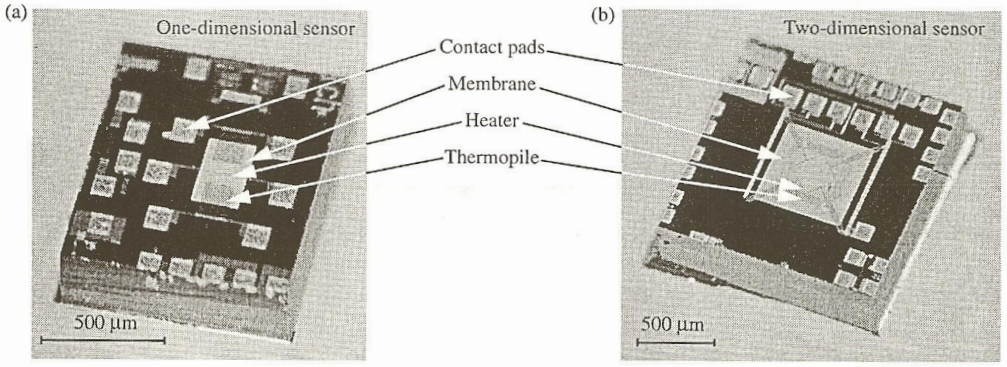

Fig. 4: Optical micrographs of the one-dimensional (a) and two-dimensional (b) CMOS air flow sensor chips.

4. ENCAPSULATION

Packaging a microsensor is a delicate issue because the encapsulation has to fulfill conflicting requirements. On one hand the protection of the device against adverse environmental influences has to be guaranteed. Simultaneously the parameter to be measured has to be focussed onto the sensor area. In the case of CMOS anemometers, this requires the package to guide the air flow to the die surface without inducing undesired turbulence, while protecting the fragile membrane against the direct contact with, e.g., the user. Ideally these constraints should be reconciled by a low-cost solution.

We have used a packaging method based on standard TO substrates and dedicated encapsulation techniques. The procedure is illustrated in Fig. 5 with the example of a one-dimensional anemometer. First, the die is glued and wire-bonded to a

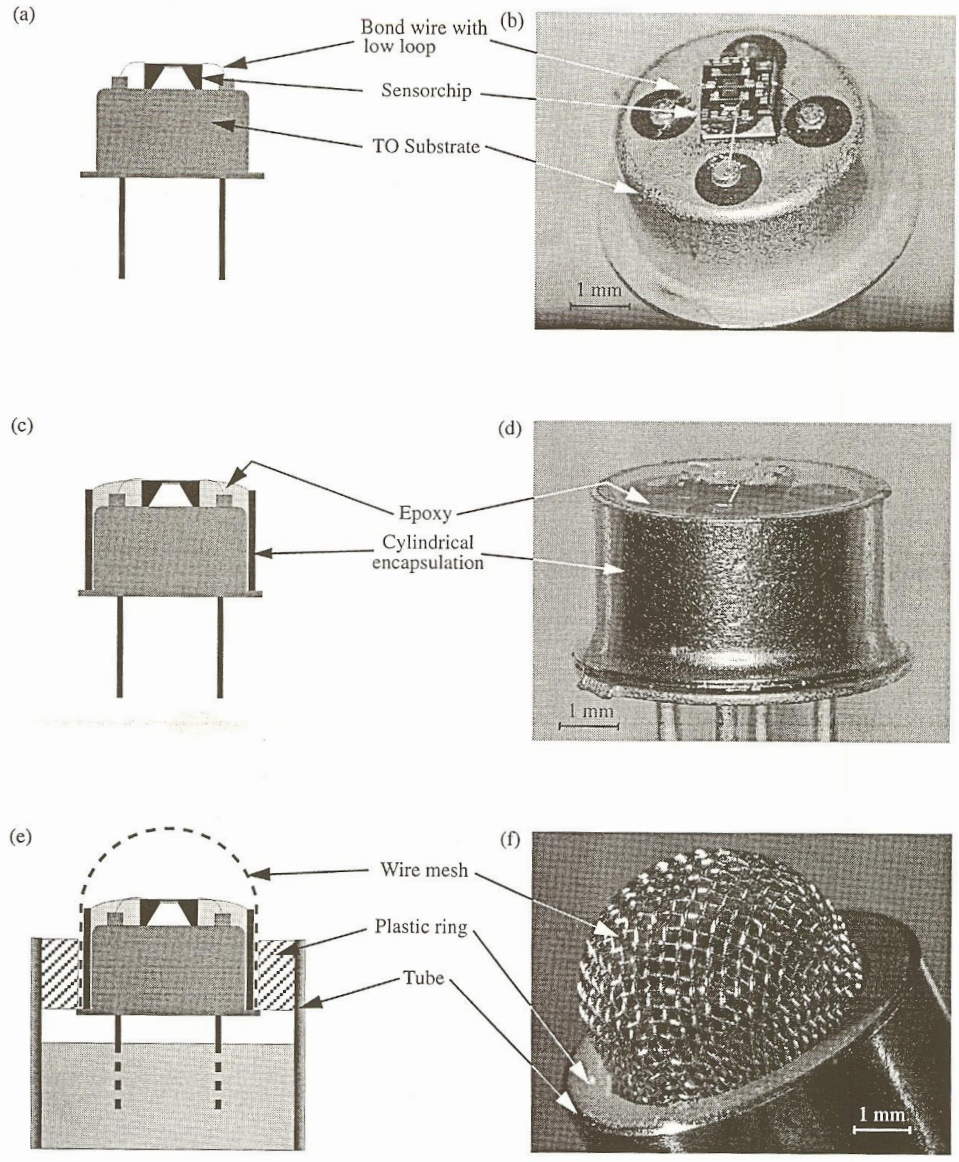

Fig. 5: Packaging of CMOS air flow sensors for anemometry. A sensor chip is glued onto a TO substrate and wire-bonded with low loop position ((a) and (b)). A cylindrical encapsulation is placed over the substrate and filled with epoxy ((c) and (d)). A hemispherical wire mesh is pushed over the TO package ((e) and (f)). The photographs show the example of a one-dimensional sensor in a TO-72 substrate.

TO-72 substrate. The wire bonding is performed with low loop, guaranteeing the smoothest possible device surface (Figs. 5 (a) and (b)). Next a cylindrical encapsulation obtained from the original TO-72 cap by cutting off its lid is placed on the substrate. The rim of the encapsulation cylinder is level with the die surface. The space between die and cylinder is then filled with UV-curable epoxy. This fixes the cylinder to the substrate and provides a smooth overall device surface (Figs. 5 (c) and (d)). Due to capillary forces, the epoxy is drawn along the bond wires to the bond pads. This embeds the wires in a solid matrix and attaches them firmly to the die surface.

Finally, the TO-72 substrate is covered with a hemispherical stainless steel wire mesh, as shown in Figs. 5 (e) and (f). Different wire meshes available from G. Bopp AG Metallgewebefabrik, Switzerland, were investigated. Relevant parameters are listed in Table 1. Mesh wire diameters ranged from 51 to 20 µm and wire densities were between 70 and 137 cm^{-1}. The meshes were preshaped by deep-drawing. They were pushed over the encapsulation cylinder and held in place with a plastic ring and stainless steel tube.

Mesh	Wire diameter [µm]	Wire density [cm^{-1}]	Fill factor [%]	Mesh thickness [µm]
G 130/51	51	70	48	110
G 40/23	23	159	60	48
G 32/25	25	180	68	54
G 53/20	20	137	47	42

Table 1: Parameters of stainless steel meshes used for the mechanical protection of CMOS anemometers.

The two-dimensional sensor was encapsulated using a similar method. A standard TO-5 substrate was used as a base. The sensor is protected by a cylindrical wire mesh of type G130/51 (cf. Table 1). A flow concentrator consisting of two conical plastic parts enhances the device performance. It surrounds the cylindrical mesh respectively above and below the sensor position. A sensor on a TO-5 substrate, embedded in epoxy, and the final encapsulation are shown in Figs. 6 (a) and (b), respectively.

Deep-drawing to produce the wire meshes and injection molding to encapsulate the sensors are established and cost-effective techniques for high volume production. Thus the packaging techniques presented here are suitable for industrialization.

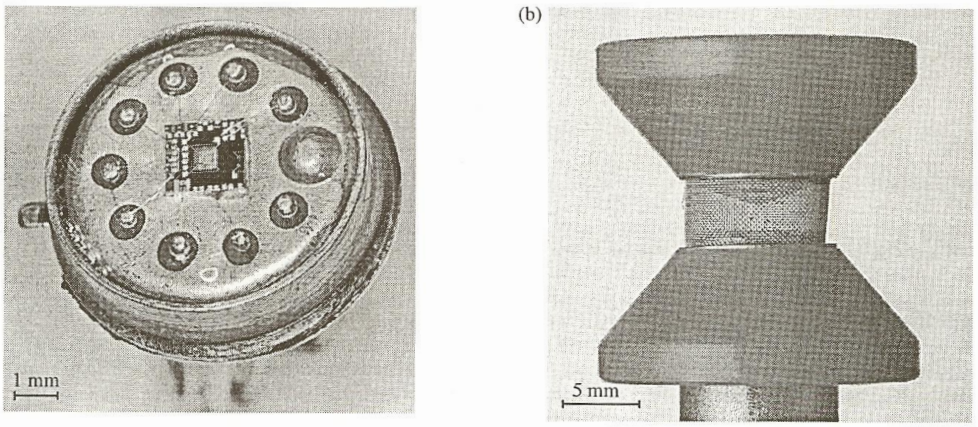

Fig. 6: (a) Sensor chip for two-dimensional wind measurements after mounting onTO-5 substrate, wire-bonding, and embedding in epoxy. (b) Encapsulation for two-dimensional anemometer with cylindrical wire mesh and flow concentrator.

5. EXPERIMENTAL

The sensors were characterized in a wind-tunnel allowing to regulate the air velocity in the range from 0 to 38 ms^{-1} (0 to 12 Beaufort). The measurements were performed in laminar flow. At the sensor location the wind-tunnel was 25 cm high and 80 cm wide. The air velocity was measured using a propeller anemometer from Schildknecht (MiniAir®2) with an accuracy better than 1.5% of the full scale output in the range from 1 to 40 ms^{-1}.

The packaged sensors were mounted on a 12 cm long rod and placed in the wind-tunnel. Two computer controlled DC motors allowed the orientation of the rod, and thus of the sensor, to be varied with respect to the air flow direction. The azimuthal orientation angle Φ of the sensor was set by rotating the rod about its axis, between 0 and 360°. Second, the inclination angle Θ of the sensor was varied between 45° (towards flow) and -45° (away from flow). The two rotations are shown in Fig. 7.

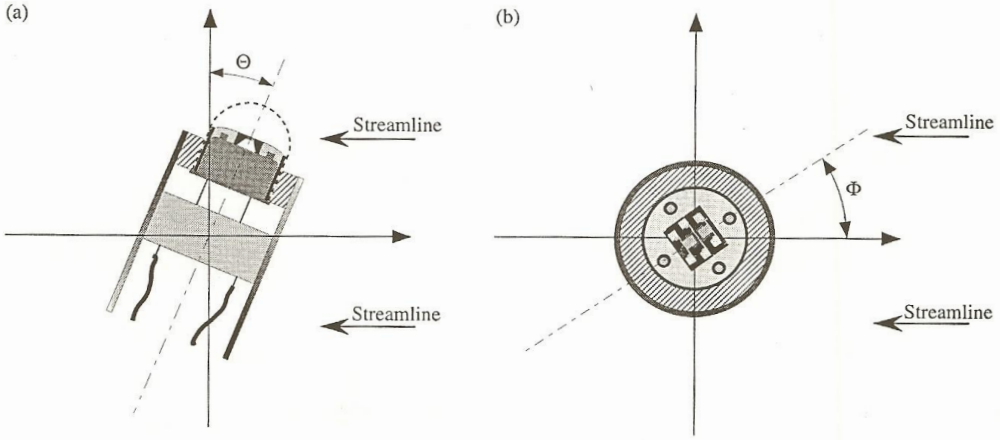

Fig. 7: Definition of sensor orientation angles with respect to flow direction. (a) Side view showing the inclination angle Θ; (b) top view showing azimuthal angle Φ.

6. RESULTS

6. 1 One-dimensional sensor

We determined the dependence of the sensor response on air flow velocity, mesh parameters (cf. Table 1), and sensor orientation. Fig. 8 shows the sensor output voltage U as a function of the azimuthal angle Φ and the inclination Θ at a flow velocity v of 5.6 ms^{-1}. The sensor was protected by mesh G40/23. At inclinations close to the horizontal position ($\Theta = 0°$), small and even negative sensor signals are observed. With increasing inclination, the signal grows and reaches a maximum close to $\Theta = 45°$. Air is injected more efficiently into the hemispherical mesh at steeper angles, and boundary layer delamination occurring at shallow angles is suppressed. At this optimum inclination, the dependence of the sensor output signal on the azimuthal angle Φ is weak, with a maximum close to $\Phi = 0°$. The signal follows a $\cos(\Phi)$ law, in agreement with the expectation that the sensor probes the velocity component parallel to its thermopiles. At smaller inclinations, irregularities of the encapsulation, such as bond wires, the irregular device surface, and variable mesh wire pitch effectively deflect the flow and cause larger deviations from the cosine.

Fig. 9 shows the sensor signal at the optimum inclination as a function of the air velocity v. The sensor was encapsulated using three meshes with fill factors of 47, 60, and 68%, respectively. For comparison, the output voltage of the unprotected

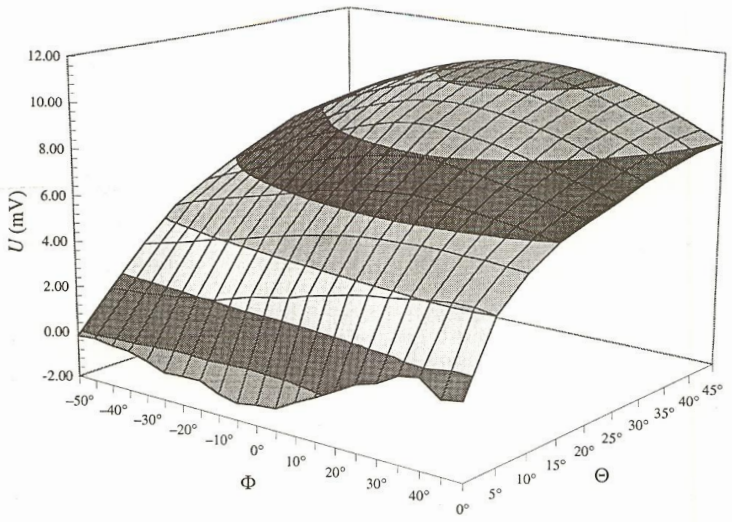

Fig. 8: Sensor output voltage U of one-dimensional anemometer as a function of azimuthal angle Φ and inclination angle Θ. Air velocity is 5.6 ms^{-1}. Sensor is protected by mesh G 40/23.

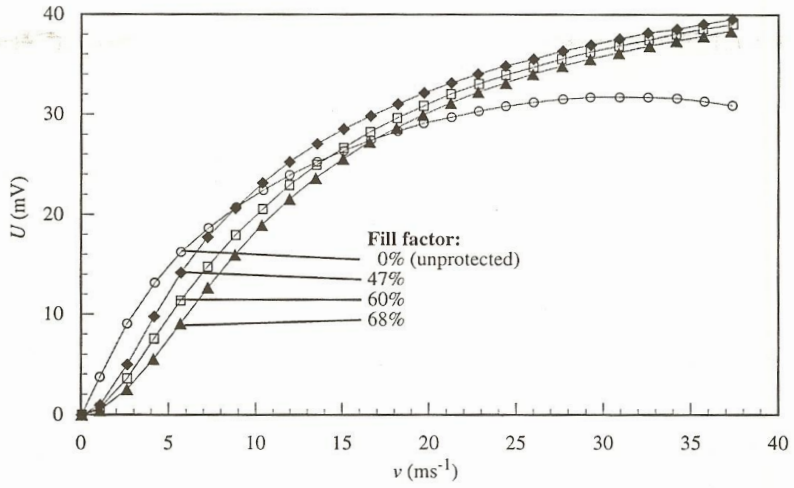

Fig. 9: Sensor output voltage U of one-dimensional anemometer as a function of the air velocity v, without mesh (○) and with meshes G 53/20 (◆), G 40/23 (□), and G 32/25 (▲). Orientation: Φ = 0°, Θ = 45°.

sensor (without mesh) is also shown. At small velocities, the response of the unprotected device is a linear function of v. At higher velocities, the signal levels off and finally decreases. In contrast, the presence of a mesh, changes the output signal into a function of v monotonically increasing over the full range. As the fill factor of the mesh is increased, the signal is progressively reduced. At air velocities above 10 ms^{-1}, the relative influence of the fill factor on the output signal drops below 10%.

6. 2 Two-dimensional sensor

Since the two-dimensional sensor is intended to measure the wind direction, $\Theta = 0^o$ (horizontal) is its natural orientation. Fig. 10 shows the experimental thermopile signals U_x and U_y of this device as a function of the azimuthal angle Φ for Θ values of 0^o and $\pm 30^o$, at a flow velocity of 5.6 ms^{-1}. As expected the thermopile signals roughly follow harmonic functions. Deviations from sin(Φ) and cos(Φ) are due to the nonlinearity of $U_x(v)$ and $U_y(v)$ and irregularities of the encapsulation. In particular, the kink close to $\Phi = 180^o$ correlates with the overlapping seam of the cylindrical mesh. Different off-vertical inclinations Θ were investigated and two of them reported in Fig. 10 to ensure that a misalignment of the device with respect to the vertical causes only negligible variations of the measured flow velocity and direction. The influence of Θ on the thermovoltages is smaller than 5% of the maximum output for inclinations between 0 and 30^o and below 15% for inclinations between 0° and -30°. An experimental azimuthal angle Φ_{exp} was determined from the data in Fig. 10, using the approximation $\Phi_{exp} = \arctan(U_y / U_x)$. The result is shown in Fig. 11. The standard deviation of Φ_{exp} from the true Φ is 10^o, 1.5^o, and 13^o, respectively, for inclinations of 30^o, 0^o, and -30^o.

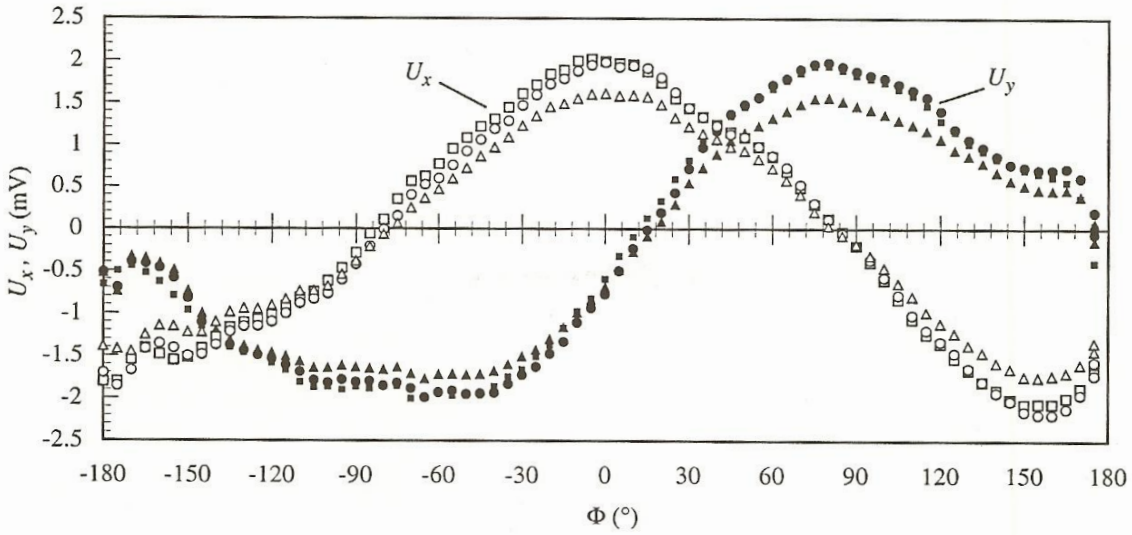

Fig. 10: Output voltages U_x and U_y of both orthogonal thermopile pairs of two-dimensional anemometer as a function of flow direction Φ for inclinations Θ of 30° (▲,△), 0° (●,○), and −30° (■,□).

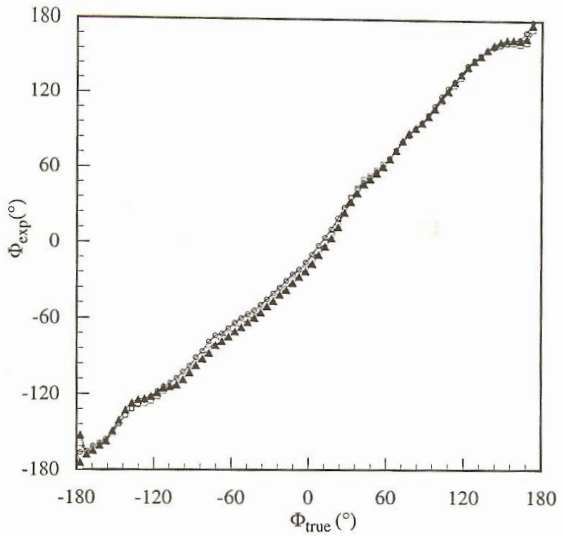

Fig. 11: Experimental flow direction Φ_{exp} versus true flow direction Φ for inclinations Θ of 30° (▲), 0° (○), and –30° (□). Φ_{exp} was calculated with data of Fig. 10.

7. CONCLUSION

We have reported packaged, miniaturized anemometers for one- and two-dimensional air flow measurements. Both are based on a thermoelectric microsensor fabricated using a commercial CMOS process and silicon bulk micromachining. The sensitivity of thermal CMOS microsensors is high enough for the measurement of free air flow.

Both devices were mounted on standard TO substrates. The one-dimensional device was protected by a hemispherical wire mesh. It showed maximum output signals if inclined by 45° towards the air flow. Air velocity measurements are possible over the entire range from still air to hurricane conditions (38 ms^{-1}). Signal levels are between 0 and 50 mV. The two-dimensional sensor was surrounded by a cylindrical mesh and built into a conical flow concentrator which strongly reduced the inclination dependence of the sensor output. It provides output voltages up to 5 mV. Flow direction measurements were demonstrated with a standard deviation smaller than 13° for inclinations between -30 and 30°.

The integration of the reported sensors with dedicated driving and read-out circuitry for linearization and temperature and offset compensations is straightforward. This possibility combined with the results reported here pave the way to small and inexpensive integrated CMOS anemometer microsystems.

8. ACKNOWLEDGMENTS

We would like to thank Prof. Dr. T. Fannelop and Mr. P. Weber for permitting the use of the wind-tunnel. We also wish to acknowledge the fabrication of the CMOS chips by Microelectronic-Marin SA, Switzerland. This work was supported by the Swiss Bundesamt für Bildung und Wissenschaft through grant Nr. 93.0161 and by the Swiss Foundation for Microelectronic Research (FSRM).